C−H Bond Activation by a Hydrotris(pyrazolyl)borato Ruthenium Hydride Complex

Siu Man Ng,[†] Wai Han Lam,[‡] Chi Chuen Mak,[†] Chun Wai Tsang,*[,†] Guochen Jia,*[,‡] Zhenyang Lin,*[,‡] and Chak Po Lau*[,†]

Department of Applied Biology and Chemical Technology, The Hong Kong Polytechnic University, Hung Hom, Kowloon, Hong Kong, China, and Department of Chemistry, The Hong Kong University of Science and Technology, Clear Water Bay, Kowloon, Hong Kong, China

Received October 30, 2002

The ruthenium complex $TpRu(PPh_3)(CH_3CN)H$ (Tp = hydrotris(pyrazolyl)borate) catalyzes H/D exchange between CH_4 and some deuterated organic solvents—benzene-d_6, tetrahydrofuran-d_8, diethyl ether-d_{10}, and dioxane-d_8. Preferential cleavage of the α-C−D and the β-C−D bonds of THF-d_8 and diethyl ether-d_{10}, respectively, is observed. The H/D exchange processes have been investigated by density functional theory calculations at the B3LYP level. Theoretical study on the reaction mechanism suggests that σ-complexes $TpRu(PPh_3)(\eta^2\text{-H−R})H$ are active species in the exchange processes. During the exchange processes, the reversible transformations of $TpRu(PPh_3)(\eta^2\text{-H−R})H$ to $TpRu(PPh_3)(\eta^2\text{-H}_2)R$ are the crucial steps. The barriers for the transformations are in the range 10−13.4 kcal/mol. Interestingly, the transition states for the transformations correspond to the seven-coordinate $TpRu(PPh_3)(R)(H)(H)$, which are species derived from the oxidative addition of H−R to the metal center. The exchange processes involve transformations of the $(\eta^2\text{-H−R})$ species to the $(\eta^2\text{-H}_2)$ species followed by H−H rotation in the latter. The rotation barriers are calculated to be in the range 2−4 kcal/mol. The exchange process having an aromatic R group is found to be most favorable due to the strong $Ru-C(sp^2)$ bonding, which stabilizes the $(\eta^2\text{-H}_2)$ species and lowers the transformation barrier. The complex $TpRu(PPh_3)(CH_3CN)H$ catalyzes H/D exchange between H_2 and the deuterated solvents too.

Introduction

The activation of molecules by transition metal complexation of σ-bonds is of fundamental interest.[1] While a large number of dihydrogen σ-complexes[2] and silane σ-complexes[3] have been isolated and/or characterized, for the moment isolable or directly observed (for example, by NMR spectroscopy) nonagostic alkane σ-complexes are extremely rare.[4] However, there is now substantial evidence in the literature for the existence of alkane (arene) σ-complexes as intermediates along the reaction pathway for C−H bond cleavage by transition metal complexes and for reductive elimination of alkyl (aryl) metal hydride complexes.[5] From the alkane (arene) σ-complex intermediates, C−H bond cleavage can be achieved either via oxidative addition to the metal center or via four-center σ-bond metathesis. C−H activation at Pt(II) centers has been extensively studied in order to gain more understanding of the mechanistic features of the Shilov system; support has been presented for a pathway in which activation of a C−H bond occurs by oxidative addition to the Pt(II) center in model systems.[6] It is also probably true that the unusually mild and selective C−H activation with the Ir(III) system $Cp^*Ir(PMe_3)(CH_3)^+$ proceeds via the oxidative addition mechanism too.[7] On the other hand, four-center σ-bond metathesis involving 1,2-addition of C−H across a metal−ligand bond in high-valent electrophilic complexes could be exemplified by C−H activation by f-element and early transition metal complexes[8] and more recently by silica-supported early transition metal

[†] The Hong Kong Polytechnic University.
[‡] The Hong Kong University of Science and Technology.

(1) (a) Crabtree, R. H. *Angew. Chem., Int. Ed. Engl.* **1993**, *32*, 789. (b) Schneider, J. J. *Angew. Chem., Int. Ed. Engl.* **1996**, *35*, 1068.
(2) Heinekey, D. M.; Oldham, W. J., Jr. *Chem. Rev.* **1993**, *93*, 3. 913. (b) Jessop, P. G.; Morris, R. H. *Coord. Chem. Rev.* **1992**, *121*, 155.
(3) Corey, J. Y.; Braddock-Wilking, J. *Chem. Rev.* **1999**, *99*, 175.
(4) Geftakis, S.; Ball, G. E. *J. Am. Chem. Soc.* **1998**, *120*, 9953.
(5) (a) Wick, D. D.; Reynolds, K. A.; Jones, W. D. *J. Am. Chem. Soc.* **1999**, *121*, 3974. (b) Flood, T. C.; Janak, K. E.; Iimura, M.; Zhen, H. *J. Am. Chem. Soc.* **2000**, *122*, 6783. (c) Johansson, L.; Tilset, M.; Labinger, J. A.; Bercaw, J. E. *J. Am. Chem. Soc.* **2000**, *122*, 10846. (d) Johansson, L.; Tilset, M. *J. Am. Chem. Soc.* **2001**, *123*, 739. (e) Northcutt, T. O.; Wick, D. D.; Vetter, A. J.; Jones, W. D. *J. Am. Chem. Soc.* **2001**, *123*, 7257.
(6) (a) Stahl, S. S.; Labinger, J. A.; Bercaw, J. E. *J. Am. Chem. Soc.* **1996**, *118*, 5961. (b) Wick, D. D.; Goldberg, K. I. *J. Am. Chem. Soc.* **1997**, *119*, 10235. (c) Holtcamp, M. W.; Henling, L. M.; Day, M. W.; Labinger, J. A.; Bercaw, J. E. *Inorg. Chim. Acta* **1998**, *270*, 467. (d) Johansson, L.; Ryan, O. B.; Tilset, M. *J. Am. Chem. Soc.* **1999**, *121*, 1974. (e) Mylvaganam, K.; Bacskay, G. B.; Hush, N. S. *J. Am. Chem. Soc.* **2000**, *122*, 2041. (f) Heiberg, H.; Johansson, L.; Gropen, O.; Ryan, O. B.; Swang, O.; Tilset, M. *J. Am. Chem. Soc.* **2000**, *122*, 10831.
(7) (a) Arndtsen, B. A.; Bergman, R. G. *Science* **1995**, *115*, 1970. (b) Strout, D. L.; Zarić, S.; Niu, S.; Hall, M. B. *J. Am. Chem. Soc.* **1996**, *118*, 6068. (c) Su, M.-D.; Chu, S.-Y. *J. Am. Chem. Soc.* **1997**, *119*, 5373. (d) Niu, S.; Hall, M. B. *J. Am. Chem. Soc.* **1998**, *120*, 6169. (e) Klei, S. R.; Tilley, T. D.; Bergman, R. G. *J. Am. Chem. Soc.* **2000**, *122*, 1816.
(8) (a) Watson, P. L. *J. Chem. Soc., Chem. Commun.* **1983**, 276. (b) Watson, P. L. *J. Am. Chem. Soc.* **1983**, *105*, 6491. (c) Fendrick, C. M.; Marks, T. J. *J. Am. Chem. Soc.* **1984**, *106*, 2214. (d) Fendrick, C. M.; Marks, T. J. *J. Am. Chem. Soc.* **1986**, *108*, 425. (e) Eisen, M. S.; Marks, T. J. *Organometallics* **1992**, *11*, 3939. (f) Thompson, M. E.; Baxter, S. M.; Bulls, A. R.; Burger, B. J.; Nolan, M. C.; Santarsiero, B. D.; Schaefer, W. P.; Bercaw, J. E. *J. Am. Chem. Soc.* **1987**, *109*, 203.

10.1021/om0209024 CCC: $25.00
Publication on Web 01/14/2003

Scheme 1

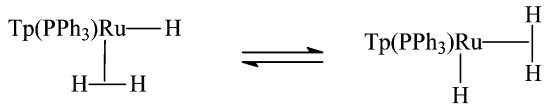

Scheme 2

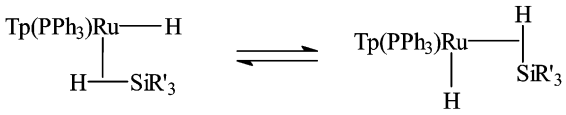

Scheme 3

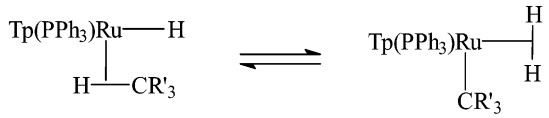

hydride complexes.[9] C−H bond cleavage is an important step for catalytic functionalization of alkanes and arenes by homogeneous transition metal complexes.[10]

We have found that the hydrotris(pyrazolyl)borato (Tp) ruthenium hydride complex $TpRu(PPh_3)(CH_3CN)H$ reacts with pressurized H_2 to give the η^2-dihydrogen complex $TpRu(PPh_3)(H_2)H$, in which rapid fluxionality exists between the hydride and the dihydrogen ligands (Scheme 1).[11] Similarly, the silane molecule can displace the acetonitrile ligand of $TpRu(PPh_3)(CH_3CN)H$ to form the highly fluxional η^2-silane complex $TpRu(PPh_3)(\eta^2\text{-}H{-}SiR'_3)H$ (Scheme 2).[12] We are therefore interested in studying the reaction of $TpRu(PPh_3)(CH_3CN)H$ with $R'_3C{-}H$, which is isolobal to H−H and $R'_3Si{-}H$. It is unlikely that an isolable or directly observable η^2-$R'_3C{-}H$ complex analogous to the η^2-H_2 and η^2-$R'_3Si{-}H$ complexes would be obtainable, but we expect that formation of a transient σ-complex of $R'_3C{-}H$ is possible and that it may equilibrate with its η^2-H_2 tautomer (Scheme 3). Such equilibrium has important implications because it represents C−H bond cleavage via abstraction of a proton by a hydride to give a dihydrogen complex. Albéniz and Crabtree first suggested that in the reversible metalation of an agostic C−H of the 2,6-diarylpyridine ligand in an iridium complex the exchange reaction proceeds via a η^2-H_2 complex, which is formed by deprotonation of the agostic C−H by the hydride ligand.[13] Chaudret et al. have recently reported a novel C−H activation process in a phenylpyridine ruthenium hydride complex, involving reversible proton transfer from an agostic aromatic C−H to the hydride ligand to yield a metalated η^2-dihydrogen species.[14] Very recently, Lee and co-workers proposed the intermediacy of a η^2-H_2 species, which was formed by proton transfer from the agostic C−H bond of the 2-(dimethylamino)-pyridine ligand to a *cis*-hydride, in a double C−H activation process occurring at an iridium complex.[15]

We set out to study the interaction of $TpRu(PPh_3)(CH_3CN)H$ with CH_4 in deuterated organic solvents. Not surprisingly, we did not detect by NMR spectroscopy either one of the σ-complexes depicted in Scheme 3, but observed catalytic H/D exchange reactions between CH_4 and the deuterated solvents. Our complex, like the cationic iridium hydride system of Golden, Andersen, and Bergman, represents a rare example of late transition metal hydrides, which promote C−H activating reactions. The iridium hydride system $[Cp^*(PMe_3)IrH(ClCH_2Cl)]^+$ is able to induce alkane C−H activation at an unexpectedly high rate and surprisingly low temperature. On the basis of what they have learned about C−H activation reactions with the analogous cationic methyl species $[Cp^*(PMe_3)IrMe(ClCH_2Cl)]^+$, the authors proposed that the most likely mechanism for the C−H activation with $[Cp^*(PMe_3)IrH(ClCH_2Cl)]^+$ involves the intermediacy of the dihydrido alkyl Ir(V) species $[Cp^*(PMe_3)IrH_2R]^+$ resulting from oxidative addition of the C−H bond to the metal center. The main feature of the proposed mechanism is that the dihydrido alkyl Ir(V) intermediate undergoes elimination of R−H, but not H_2.[16] We believe that for our system the $R'_3C{-}H$ and dihydrogen σ-complexes shown in Scheme 3, rather than the C−H oxidative addition Ru(IV) species, are transient intermediates inside the catalytic cycle; however, it is true that the $R'_3C{-}H$ dissociates from the σ-$R'_3C{-}H$ intermediate more readily than H_2 from the η^2-dihydrogen intermediate under the reaction conditions. Reported here are the experimental results of the H/D exchange and the theoretical calculations that provide a better understanding of the relevant transition states and intermediates in the reaction pathway.

Results and Discussion

H/D Exchange between CH_4 and Deuterated Solvents. We monitored the reaction of $TpRu(PPh_3)(CH_3CN)H$ in benzene-d_6 with CH_4 (∼10 atm) at 100 °C in a 5 mm Wilmad pressure-valved NMR tube by ^1H NMR spectroscopy over the course of several hours. It was found that intensities of the residual peak of the deuterated solvent gradually increased and signals of the methane isotopmers (i.e., CH_3D, CH_2D_2, and CHD_3) grew in at the expense of the intensity of the CH_4 peak. This phenomenon is indicative of H/D exchange between methane and benzene-d_6. Unexpectedly, the proton signals of the phosphine and Tp ligands diminished; moreover, those of the hydride and acetonitrile ligands disappeared even more rapidly. Diminution and disappearance of the proton peaks of the ligands signal H/D exchange between the deuterated solvent and the ligands too, suggesting that $TpRu(PPh_3)(CH_3CN)H$

(9) (a) Corker, J.; Lefebvre, F.; Lécuyer, C.; Dufaud, V.; Quignard, F.; Choplin, A.; Evans, J.; Basset, J.-M. *Science* **1996**, 966. (b) Vidal, V.; Théolier, A.; Thivolle-Cazat, J.; Basset, J.-M. *Science* **1997**, 99. (c) Maury, O.; Lefort, L.; Vidal, V.; Thivolle-Cazat, J.; Basset, J.-M. *Angew. Chem., Int. Ed.* **1999**, *38*, 1952. (d) Lefort, L.; Copéret, C.; Taoufik, M.; Thivolle-Cazat, J.; Basset, J.-M. *Chem. Commun.* **2000**, 663. (e) Casty, G. L.; Matturro, M. G.; Myers, G. R.; Reynolds, R. P.; Hall, R. B. *Organometallics* **2001**, *20*, 2246.

(10) (a) Arndtsen, B. A.; Bergman, R. G.; Mobley, T. A.; Peterson, T. H. *Acc. Chem. Res.* **1995**, *28*, 154. (b) Crabtree, R. H. *Chem. Rev.* **1995**, *95*, 987. (c) Hall, C.; Perutz, R. N. *Chem. Rev.* **1996**, *96*, 3125. (d) Guari, Y.; Sabo-Etienne, S.; Chaudret, B. *Eur. J. Inorg. Chem.* **1999**, 1047.

(11) Chen, Y.-Z.; Chan, W. C.; Lau, C. P.; Chu, H. S.; Lee, H. L.; Jia, G. *Organometallics* **1997**, *16*, 1241.

(12) Ng, S. M.; Lau, C. P.; Fan, M. F.; Lin, Z. *Organometallics* **1999**, *18*, 2484.

(13) Albéniz, A. C.; Schulte, G.; Crabtree, R. H. *Organometallics* **1992**, *11*, 242.

(14) Toner, A. J.; Gründemann, S.; Clot, E.; Limbach, H.-H.; Donnadieu, B.; Sabo-Etienne, S.; Chaudret, B. *J. Am. Chem. Soc.* **2000**, *122*, 6777.

(15) Lee, D.-H.; Chen, J.; Faller, J. W.; Crabtree, R. H. *Chem. Commun.* **2001**, 213.

(16) Golden, J. T.; Andersen, R. A.; Bergman, R. G. *J. Am. Chem. Soc.* **2001**, *123*, 5837.

Table 1. Distribution of Methane Isotopomers Resulting from $TpRu(PPh_3)(CH_3CN)H$-Catalyzed H/D Exchange Reactions between CH_4 and the Deuterated Solvents[a]

		methane isotopomers (%)[b]						
entry	solvent	CH_4	CH_3D	CH_2D_2	CHD_3	CD_4	TON[c]	selectivity[d]
1	C_6D_6	17	39	32	10	2.0	63	
2	THF-d_8	49	39	11	1.0	ND[f]	29	α C−D/β C−D = 3.2
3	dioxane-d_8	75	19	5.0	1.0	ND[f]	15	
4[e]	diethyl ether-d_{10}	93	5.0	2.0	ND[f]	ND[f]	16	α C−D/β C−D = 0.4

[a] Reaction conditions: catalyst, 6.7 μmol; deuterated solvent, 0.3 mL; CH_4, 8 atm at room temperature; CH_4:$TpRu(PPh_3)(CH_3CN)H \approx$ 45:1. Reaction temperature, 100 °C; reaction time, 14 h. [b] Determined by MS. [c] Mol of C−H bond activated/mol of catalyst. [d] Estimated from intensities of the residual solvent peaks. [e] Catalyst, 1.7 μmol. [f] ND = not detected.

might be an efficient catalyst for some other intermolecular H/D exchange reactions. There are in fact precedents of this type of H/D exchange between deuterated solvent and the ligands of the complex in the literature.[17] Realizing that $TpRu(PPh_3)(CH_3CN)H$ is capable of catalyzing H/D exchange between CH_4 and benzene-d_6, we studied the catalysis in some deuterated organic solvents in a more quantitative manner. In a typical H/D exchange experiment, a solution of $TpRu(PPh_3)(CH_3CN)H$ in the deuterated solvent was pressurized with 8 atm of CH_4 in a 5 mm Wilmad pressure-valved NMR tube at room temperature. After heating the solution at 100 °C for 14 h, the gases in the headspace of the tube were analyzed by electron-impact ionization mass spectrometry. Distributions of the methane isotopomers in the catalytic reactions are listed in Table 1; selectivity in C−D bond activation can be seen in THF-d_8 and diethyl ether-d_{10}. Due to extensive H/D exchange between the ligands of the complex and the solvent, the signals in the ^1H NMR spectrum of the recovered residue at the end of the catalysis were very weak. Therefore little information on the nature of the recovered metal-containing species could be obtained. In a set of controlled experiments, solutions of $TpRu(PPh_3)(CH_3CN)H$ in nondeuterated solvents were heated under conditions identical to those of the H/D exchange processes of Table 1; ^1H and $^{31}P\{^1H\}$ NMR spectra of the recovered residue showed that in each case, in addition to $TpRu(PPh_3)(CH_3CN)H$, small amounts of the known complex $TpRu(PPh_3)_2H$[18] and unidentified species were present. Prolonged heating (4 days) of the solutions eventually gave unidentified species, which were proved to be inactive for H/D exchange reactions between CH_4 and deuterated solvents.

Possible Mechanisms of H/D Exchange Reactions. In view of the propensity of the $Tp(PPh_3)RuH$ fragment to form σ-complexes with H_2[11] and silane[12] and the strong preference of Tp ligands for octahedral geometry about the metal center,[19] we propose a reaction sequence for the H/D exchange between CH_4 and the deuterated solvent R−D (Scheme 4). The main

Scheme 4

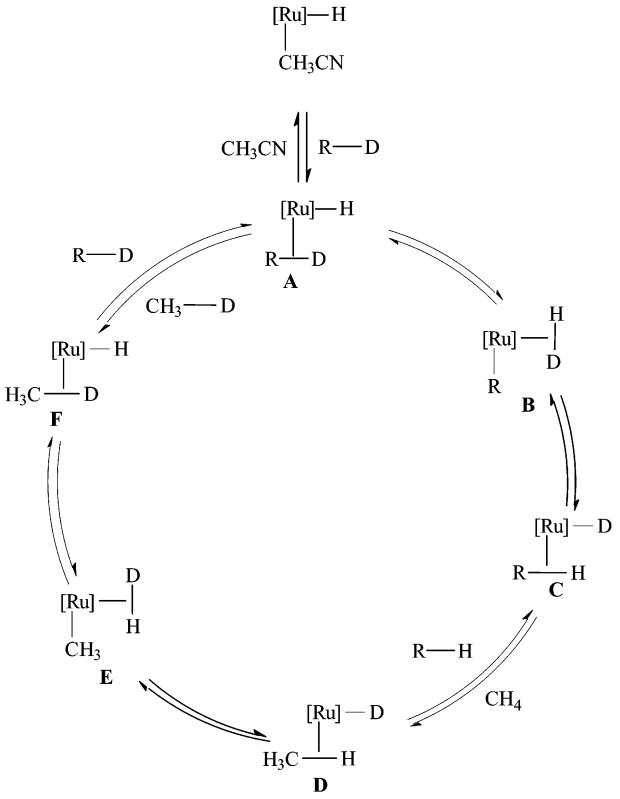

[Ru] = $TpRu(PPh_3)$

feature of this proposed catalytic cycle is the presence of equilibrating σ-complexes. Ru−H and the deuterated solvent molecule (R−D) first undergo H/D exchange via the intermediacies of σ-complexes **A**−**C**; Ru−D then undergoes H/D exchange with CH_4 in a similar manner. It is proposed in Scheme 4 that the η^2-HD intermediates are results of net proton transfer from the coordinated C−D (C−H) to the neighboring hydride (deuteride) ligand. The reverse of the η^2-HD species-generating step in Scheme 4 is a hydrogenolysis reaction, which is believed to be the product-generating step in some transition metal-catalyzed olefin hydrogenation reactions.[20] The intimate mechanism of interconversion between each pair of σ-complexes is not shown in Scheme 4; for example, conversion of **A** to **B** might proceed via oxidative addition of R−D to the metal and subsequent coupling of the hydride and deuteride ligands to give the η^2-HD ligand in **B**. It might also proceed via a four-center σ-bond metathesis pathway.

(17) For examples: (a) Cameron, C. J.; Felkin, H.; Fillebeen-Khan, T.; Forrow, N. J.; Guittet, E. *J. Chem. Soc., Chem. Commun.* **1986**, 801. (b) Chaudret, B. *J. Organomet. Chem.* **1984**, *268*, C33. (c) Perthuisot, C.; Fan, F.; Jones, W. D. *Organometallics* **1992**, *11*, 3622. (d) Djurovich, P. I.; Carroll, P. J.; Berry, D. H. *Organometallics* **1994**, *13*, 2551.

(18) Chan, W. C.; Lau, C. P.; Chen, Y.-Z.; Fang, Y.-Q.; Ng, S. M.; Jia, G. *Organometallics* **1997**, *16*, 34.

(19) (a) Curtis, M. D.; Shiu, K.-B.; Butler, W. M. *J. Am. Chem. Soc.* **1986**, *108*, 1550. (b) Curtis, M. D.; Shiu, K.-B.; Butler, W. M.; Huffman, J. C. *J. Am. Chem. Soc.* **1986**, *108*, 3335. (c) Gemel, C.; Trimmel, G.; Slugovc, C.; Kremel, S.; Mereiter, K.; Schmid, R.; Kirchner, K. *Organometallics* **1996**, *15*, 3998. (d) Rüba, E.; Simanko, W.; Mereiter, K.; Schmid, R.; Kirchner, K. *Inorg. Chem.* **2000**, *39*, 382. (e) Tellers, D. M.; Bergman, R. G. *Organometallics* **2001**, *20*, 4819.

(20) Crabtree, R. H. *The Organometallic Chemistry of the Transition Metals*, 3rd ed.; Wiley: New York, 2001; p 238.

Scheme 5

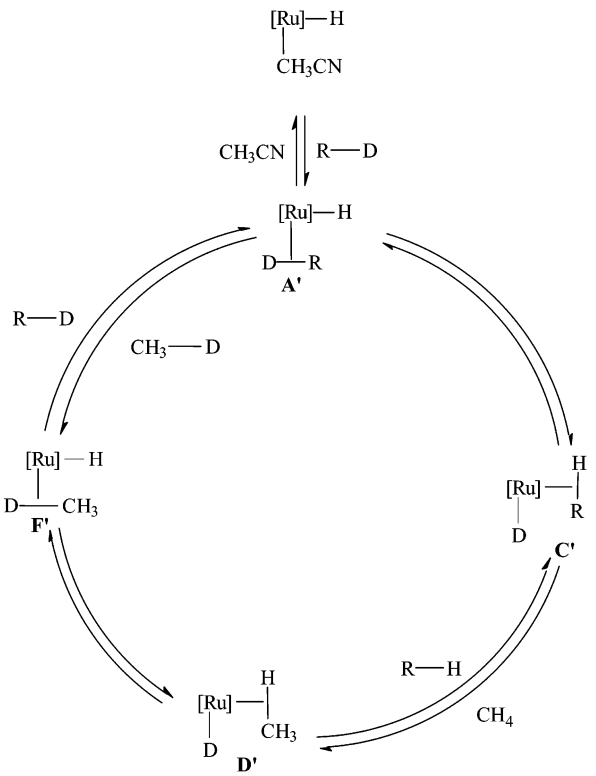

[Ru] = TpRu(PPh$_3$)

A radical mechanism for the catalytic H/D exchange can be ruled out because addition of radical quencher 2,4,6-tri-*tert*-butylphenol has little effect on the TON of the reactions. However, the presence of H_2 (4 atm) basically quenched the H/D exchange reactions between CH_4 and the deuterated solvents, but the exchange reactions occurred between H_2 and the solvents instead. In these cases, the recovered materials contained primarily TpRu(PPh$_3$)(H_2)H, and only a very minute amount of TpRu(PPh$_3$)(CH_3CN)H was present. Probably, the complex TpRu(PPh$_3$)(H_2)H, which is readily generated under catalytic conditions, is effective in catalyzing H/D exchange between H_2 and the deuterated solvents (vide infra).

Scheme 5 shows another possible scenario of the catalytic H/D exchange reactions. Although this proposed mechanism seems to provide a more direct way to accomplish H/D exchange between CH_4 and the deuterated solvents, it is shown by theoretical study that it is indeed not a favorable one (vide infra).

In the exchange reactions involving deuterated ethers, C−D σ-complexes are probably the major active species in the H/D exchange cycle, although oxygen bonding of the ethers to the metal center is also possible. However, direct H/D exchange at the O-bonded complexes would likely require much higher activation energies (vide infra). It was postulated that selectivity in H/D exchange between THF (α-C−H) and C_6D_6 catalyzed by a neutral manganese complex was attributable to heteroatom precoordination of THF to the metal center.[17c] In the electrophilic organometallic complex $[Cp^*W(CO)_3(OEt_2)]^+$-BAr_4^- (Ar = 3,5-bis(trifluoromethyl)phenyl), in which the ether molecule is O-bonded, the electron-withdrawing effect of the cationic tungsten center through the oxygen atom facilitates the α-C−H bond activation, so that nucleophilic and sterically demanding tertiary phosphines react at the α-carbon of Et_2O and transfer the α-hydrogen to the tungsten center, yielding $Cp^*W(CO)_3H$ and the phosphonium salts $Et_2OCH(Me)PR_3^+BAr_4^-$ (R = Ph, Cy).[21] In our case, the α-C−D bonds of THF-d_8 and the β-C−D bonds of diethyl ether-d_{10} are probably sterically more favorable in the formation of the C−D σ-complexes; therefore they become the favorable sites for H/D exchange. It is well known that double α-C−H activation (in fact, it is α-C−H activation followed by α-hydrogen migration) of cyclic and acyclic ethers by transition metal complexes leads to the formation of Fisher type metal carbenes.[22] β-C−H activation of Et_2O by a iridium complex and subsequent β-hydrogen migration to give an η^2-vinyl ether complex has been reported.[7a,22d]

H/D Exchange between H_2 and Deuterated Solvents. Table 2 shows the results of H/D exchange between H_2 and the deuterated solvents in the presence of TpRu(PPh$_3$)(CH_3CN)H. In each of the catalytic reactions, H_2 was converted into a mixture of the isotopomers, the distributions of which were determined by mass spectrometry. Again, selectivities similar to those observed in H/D exchange between CH_4 and deuterated solvents were observed for C−D activation in THF-d_8 and diethyl ether-d_{10}. A reaction mechanism for the catalytic H/D exchange between H_2 and the deuterated solvents (R−D), which is similar to that for the catalytic H/D exchange between CH_4 and R−D, is depicted in Scheme 6. The resting state of the catalyst in this case is the η^2-dihydrogen complex TpRu(PPh$_3$)(H_2)H, which is readily formed by displacement of the CH_3CN ligand of TpRu(PPh$_3$)(CH_3CN)H by H_2 under the catalytic conditions. As mentioned above, the presence of H_2 (4 atm) basically quenched the TpRu(PPh$_3$)(CH_3CN)H-catalyzed H/D exchange reactions between CH_4 and the deuterated solvents, and the H/D exchange reactions occurred between H_2 and the solvents instead. This fact indicates that H/D exchange between H_2 and R−D has a lower energy barrier than that between CH_4 and the solvent. Transition metal complex catalyzed H/D exchange between D_2 and aromatic hydrocarbons or between H_2 and deuterated aromatic hydrocarbons is not uncommon. For example, Klabunde and Parshall first reported H/D exchange between D_2 and substituted benzenes catalyzed by polyhydride complexes in the early 1970s,[23] Collman and co-workers learned that some electron-deficient Ru(II) porphyrins slowly catalyzed the exchange of H_2 into benzene-d_6 and toluene-

(21) Yi, C. S.; Wódka, D.; Rheingold, A. L.; Yap, G. P. A. *Organometallics* **1996**, *15*, 2.

(22) (a) Werner, H.; Weber, B.; Nürnberg, O.; Wolf, J. *Angew. Chem., Int. Ed. Engl.* **1992**, *31*, 1025. (b) Boutry, O.; Gutiérrez, E.; Monge, A.; Nicasio, M. C.; Pérez, P. J.; Carmona, E. *J. Am. Chem. Soc.* **1992**, *114*, 7288. (c) Li, Z.-W.; Taube, H. *J. Am. Chem. Soc.* **1994**, *116*, 11584. (d) Luecke, H. F.; Arndtsen, B. A.; Burger, P.; Bergman, R. G. *J. Am. Chem. Soc.* **1996**, *118*, 2517. (e) Holtcamp, M. W.; Labinger, J. A.; Bercaw, J. E. *J. Am. Chem. Soc.* **1997**, *119*, 848. (f) Gutiérrez-Puebla, E.; Monge, A.; Nicasio, M. C.; Pérez, P. J.; Poveda, M. L.; Carmona, E. *Chem. Eur. J.* **1998**, *4*, 2225. (g) Slugovc, C.; Mereiter, K.; Trofimenko, S.; Carmona, E. *Angew. Chem., Int. Ed.* **2000**, *39*, 2158. (h) Slugovc, C.; Mereiter, K.; Trofimenko, S.; Carmona, E. *Chem. Commun.* **2000**, 121.

(23) (a) Barefield, E. K.; Parshall, G. W.; Tebbe, F. N. *J. Am. Chem. Soc.* **1970**, *92*, 5234. (b) Parshall, G. W.; Klabunde, U. *J. Am. Chem. Soc.* **1972**, *94*, 9081.

Table 2. Distribution of Hydrogen Isotopomers Resulting from TpRu(PPh$_3$)(CH$_3$CN)H-Catalyzed H/D Exchange Reactions between H$_2$ and the Deuterated Solvents[a]

		hydrogen isotopomers (%)[b]				
entry	solvent	H_2	HD	D_2	TON[c]	selectivity[d]
1	C_6D_6	2	42	56	85	
2	THF-d_8	42	54	4	34	α C−D/β C−D = 2.6
3	diethyl ether-d_{10}	47	50	3	31	α C−D/β C−D = 0.3

[a] Reaction conditions: catalyst, 6.7 μmol; deuterated solvent, 0.3 mL; H_2, 10 atm at room temperature; H_2:TpRu(PPh$_3$)(CH$_3$CN)H ≈ 55:1. Reaction temperature, 100 °C; reaction time, 14 h. [b] Determined by MS. [c] Mol of H−H bond activated/mol of catalyst. [d] Estimated from intensities of the residual solvent peaks.

Scheme 6

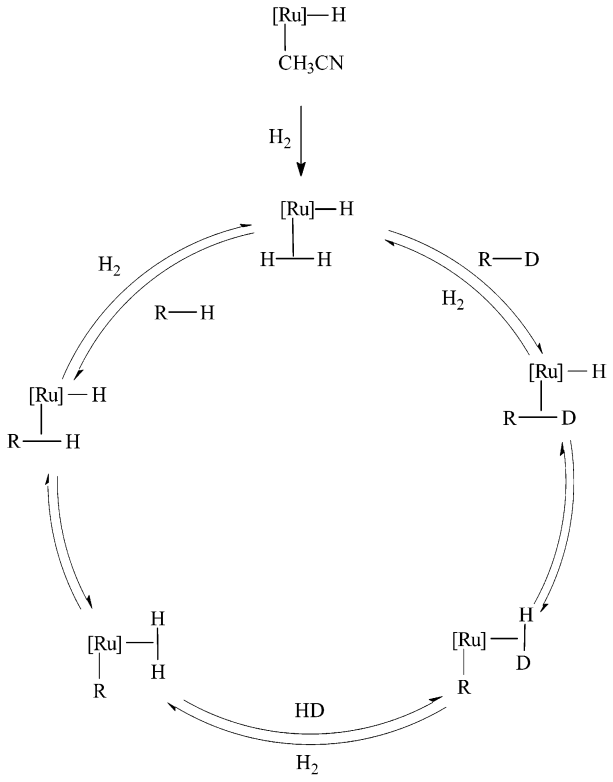

[Ru] = TpRu(PPh$_3$)

d_8,[24] and a manganese trihydride complex was found to be capable of catalyzing H/D exchange between H_2 and benzene-d_6.[17c]

Theoretical Study. To understand the relevant transition states and intermediates in the H/D exchange reactions catalyzed by TpRu(PPh$_3$)(CH$_3$CN)H, theoretical calculations at the B3LYP level of density functional theory to study a more detailed catalytic pathway were carried out. An important implication of the proposed H/D exchange mechanism shown in Scheme 4 is that nonclassical σ-complexes are active species in the reaction cycle. Another important question is whether C−H/C−D activations in the H/D exchange reaction occur through an oxidative addition pathway or via a four-center σ-bond metathesis mechanism.

To reduce the computational cost, model catalyst TpRu(PH$_3$)(CH$_3$CN)H was used in which the phenyl groups in the phosphine ligand were replaced by H atoms. Two systems were chosen for study here: the H/D exchange between CH_4 and C_6D_6, as well as the exchange between CH_4 and $CD_3CD_2OCD_2CD_3$. In our study, C_6H_6 and $CH_3CH_2OCH_2CH_3$ were used as models of deuterated solvents C_6D_6 and $CD_3CD_2OCD_2CD_3$. Therefore, the model H/D exchange system can be viewed as the hydrogen exchanges between CH_4 and C_6H_6 and exchanges between CH_4 and $CH_3CH_2OCH_2$-CH_3.

(a) Hydrogen Exchange Pathways. Before we give the detailed results of our calculations, let us re-examine Scheme 4 and see what we have focused on. The catalytic circle shown in Scheme 4 involves two types of reactions. The transformations of **A** → **B** → **C** and **D** → **E** → **F** are the H/D exchanges in σ-complexes containing Ru-η^2-(H−C). The steps of **C** → **D** and **F** → **A** are simple substitution reactions between ligands η^2-(H−CH$_3$) and η^2-(H−R) (R = −C$_6$H$_5$ or −CH$_2$CH$_2$-OC$_2$H$_5$).

It is expected that the metal−η^2-(H−R) bonds are thermally labile because the metal−η^2-(H−R) interactions should not be very strong. We can conclude that the substitution reactions involving **C** → **D** and **F** → **A** are not crucial in the catalytic circle. The two transformations (**A** → **B** → **C** and **D** → **E** → **F**) are basically the same if we consider the CH$_3$ group as an alkyl one (R). Therefore, the reactions we need to focus on are those related to **A** → **B** → **C**. In other words, hydrogen exchanges based on **A** → **B** → **C** shown in Scheme 4 will be investigated in detail for R = −CH$_3$, −C$_6$H$_5$, or −CH$_2$-CH$_2$OC$_2$H$_5$.

For the convenience of our discussion, all calculated structures of intermediates, reactants, and transition states are numbered. The numbers are then followed by bold letters, **Ph** for R = −C$_6$H$_5$, **Et*** for R = −CH$_2$-CH$_2$OC$_2$H$_5$, and **Me** for R = −CH$_3$.

Figure 1 shows the potential energy profiles of the hydrogen exchange processes for the three systems TpRu(PH$_3$)H(η^2-H−R) (R = −C$_6$H$_5$, −CH$_2$CH$_2$OC$_2$H$_5$, and −CH$_3$) investigated. In each of the three exchange processes, the starting σ-complex [Ru](H) (η^2-H−R) (**1**) (here [Ru] = TpRu(PH$_3$)) undergoes an oxidative addition, giving [Ru](H)$_2$R (**2**) as the transition state for the formation of the intermediate η^2-H_2 σ-complex **3**. The rotation of the η^2-H_2 ligand in the intermediate **3** gives the same intermediate by exchanging the positions of the two hydrogens in the η^2-H_2 ligand. The intermediate **3** then passes through the dihydride transition state **2**, completing the hydrogen exchange (see Figure 1). As mentioned above, ligand substitution reactions of **C** → **D** and **F** → **A** in Scheme 4 are not crucial in terms of energy cost in the catalytic circle. Indeed, the η^2-H−R ligand dissociation energies are found to be small, 9.0, 6.3, and 6.0 kcal/mol, respectively, for σ-complexes **1Ph**, **1Et***, and **1Me**. The ligand substitution reactions are

(24) Collman, J. P.; Fish, H. T.; Wagenknecht, P. S.; Tyvoll, D. A.; Chng, L.-L.; Eberspacher, T. A.; Brauman, J. I.; Bacon, J. W.; Pignolet, L. H. *Inorg. Chem.* **1996**, *35*, 6746.

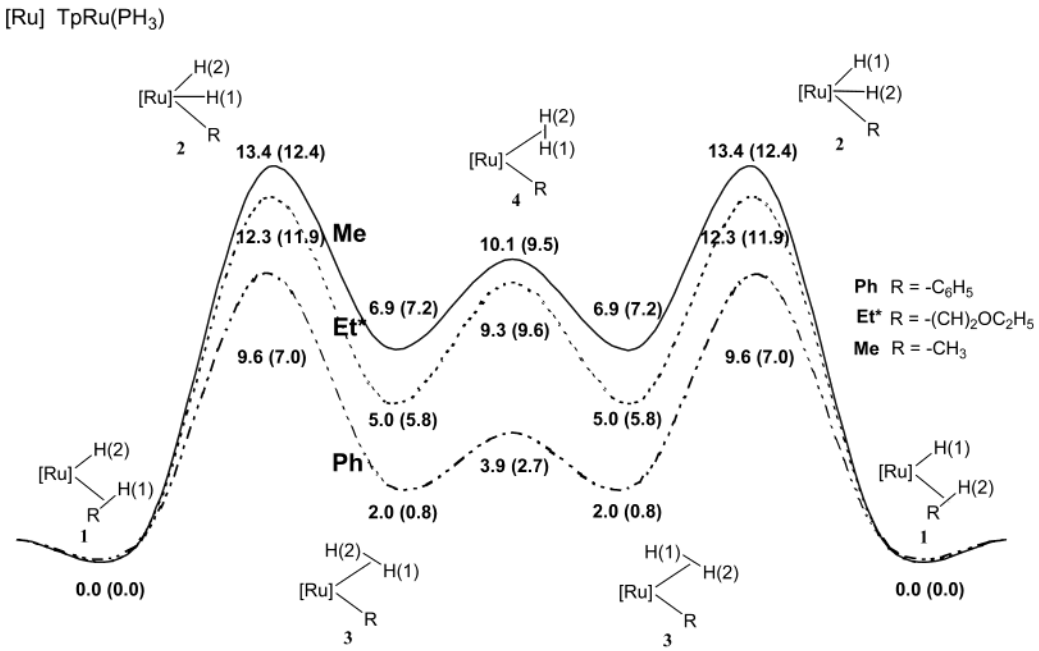

Figure 1. Potential energy profiles for hydrogen exchange reactions catalyzed by $TpRu(PH_3)H$. Pathway **Ph** represents the exchange between the hydride and hydrogens of benzene. Pathway **Et*** is for the exchange between the hydride and hydrogens of diethyl ether. Pathway **Me** gives the exchange between the hydride and hydrogens of methane. The relative reaction energies are given in kcal/mol. The values in parentheses are relative free energies.

expected to have even smaller barriers because the dissociation energies are the upper limits for the substitution reactions. Therefore, the relationship between the potential energy curves and Scheme 4, which illustrates the H/D exchange mechanistic cycle, can be described as follows. If one starts from left to right (**1** → **2** → **3** → **4** → **3** → **2** → **1**) based on curve **Ph** and then comes back from right to left based on curve **Me**, one completes the reaction circle of H/D exchange between C_6D_6 and CH_4. Similarly, the H/D exchange between $C_2D_5OC_2D_5$ and CH_4 is based on the curves **Et*** and **Me**.

From Figure 1, we can see that the barriers for the hydrogen exchange are not high. These results suggest that once the η^2-H−R complexes are formed, the relevant hydrogen exchange between the hydride and the hydrogen in the coordinated η^2-H−R ligand can easily occur. However, the formation of η^2-H−R complexes $TpRu(PH_3)H(\eta^2\text{-H}-R)$ requires the dissociation of the NCMe ligand from $TpRu(PH_3)H(NCMe)$. The dissociation energy of $TpRu(PH_3)H(NCMe) \rightarrow TpRu(PH_3)H$ + NCMe (see Figures 2a and 2b for the calculated structures) is calculated to be 28.2 kcal/mol, which is much higher than the barriers associated with the hydrogen exchange based on the η^2-H−R complexes. Clearly, the harsh experimental conditions (100 °C for several hours; it was later found out the H/D exchange reactions could proceed at 80 °C, but at lower rates) are mainly for the dissociation of the NCMe ligand. The relative stability of **1** and **3** deserves some comments here. Interestingly, the dihydrogen intermediates **3** are relatively less stable than the C−H σ-complexes **1**. At first glance, the results seem unexpected because dihydrogen complexes are usually more prevalent. The reason for the higher stability of **1** is that the metal−hydride bonds (in **1**) are stronger than the metal−alkyl (aryl) bonds (in **3**). We are comparing the stability of two tautomeric forms of the Ru complexes, not the stability of the η^2-H_2 and η^2-H−R complexes of the same metal fragment.

We can also see from Figure 1 that the benzene system has the lowest exchange reaction barriers, while methyl system has the highest. The H_2 rotational barriers for the three systems are in the range 2−4 kcal/mol, an upper bound found for other related η^2-H_2 systems.[25] Rationalization of these results will be given later.

In the discussion above, we assume that η^2-H−R complexes (**1Ph**, **1Et***, and **1Me**) are formed after dissociation of NCMe ligands. However, for the cases of benzene and ether, the coordination to the metal center after dissociation of the NCMe ligand can also be the π-electron pairs of the benzene and the lone pairs on the oxygen atom of the diethyl ether. For the benzene case, a structure (Figure 2c) having a metal-coordinated η^2-C−C unit $TpRu(PH_3)H(\eta^2\text{-}C_6H_6)$ has been optimized, and its relative energy is calculated to be slightly higher than that of the η^2-H−C complex **1Ph** (+0.7 kcal/mol). These results suggest that a fast equilibrium between the two types of coordinated complexes exists.

For the diethyl ether case, the O-bonded model complex $TpRu(PH_3)H(OC_4H_{10})$ has been optimized, and its relative energy is indeed lower by 11.5 kcal/mol than the η^2-H−R complex **1Et***. The result is expected because the oxygen atom in the diethyl ether is a better donor in comparison to the η^2-H−C bond. To facilitate the hydrogen exchange process, the O-bonded species

(25) (a) Riehl, J.-F.; Pélissier, M.; Eisenstein, O. *Inorg. Chem.* **1992**, *31*, 3344. (b) Eckert, J.; Albinati, A.; Bucher, U. E.; Venanzi, L. M. *Inorg Chem.* **1996**, *35*, 1292. (c) Bianchini, C.; Masi, D.; Peruzzini, M.; Casarin, M.; Maccato, C.; Rizzi, G. A. *Inorg. Chem.* **1997**, *36*, 1061. (d) Rodriguez, V.; Sabo-Etienne, S.; Chaudret, B.; Thoburn, J.; Ulrich, S.; Limbach, H.-H.; Eckert, J.; Barthelat, J.-C.; Hussein, K.; Marsden, C. J. *Inorg. Chem.* **1998**, *37*, 3475. (e) Gelabert, R.; Moreno, M.; Lluch, J. M.; Lledos, A. *Organometallics* **1997**, *16*, 3805. (f) Eckert, J.; Kubas, G. J.; Hall, J. H.; Hay, P. J.; Boyle, C. M. *J. Am. Chem. Soc.* **1990**, *112*, 2324.

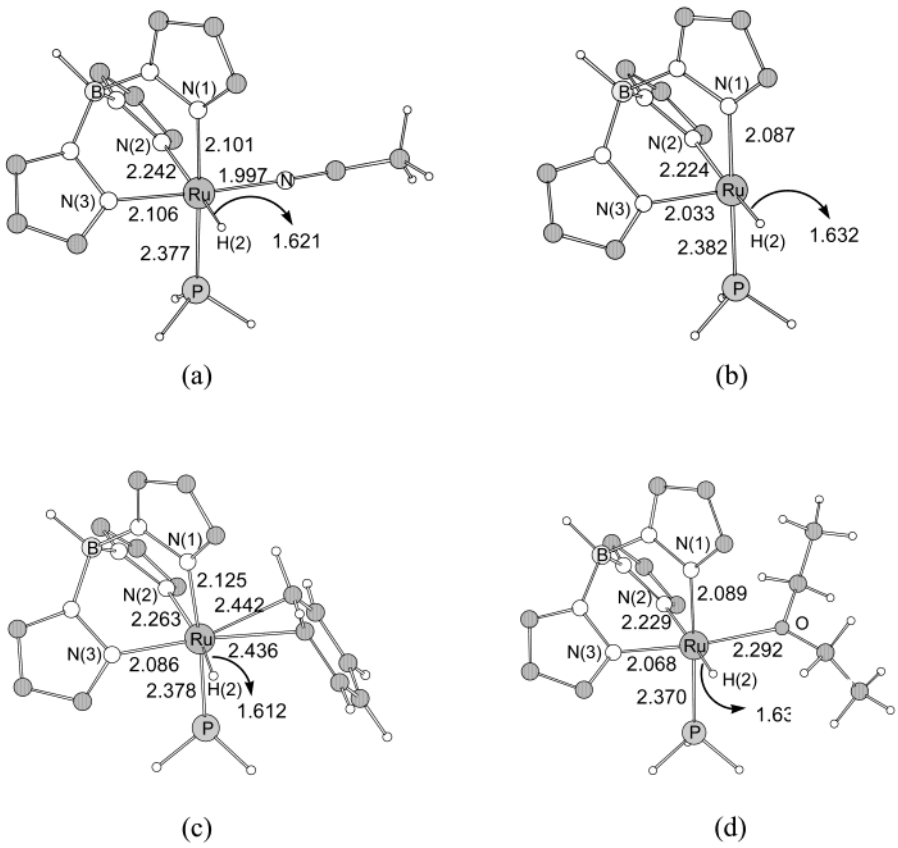

Figure 2. B3LYP optimized structures (a) TpRu(PH_3)(CH_3CN)H, (b) TpRu(PH_3)H, (c) TpRu(PH_3)H(η^2-C_6H_6), and (d) TpRu(PH_3)H(OC_4H_{10}) with their selected bond distances (Å). For the purpose of clarity, hydrogen atoms on the pyrazolyl ring are omitted.

has to undergo a coordination site exchange reaction, similar to a substitution reaction, to give the H−C coordinated complex **1Et***. A direct hydrogen exchange process at the O-bonded species is expected to have a substantial reaction barrier since the C−H bonds in such an O-bonded complex are unactivated. The energy for the dissociation of the O-bonded $CH_3CH_2OCH_2CH_3$ ligand from TpRu(PH_3)H{$O(C_2H_5)_2$} has been calculated (17.8 kcal/mol), and it can be considered as the upper limit for the barrier of the coordination site exchange. The higher stability of the O-bonded complex can explain the significantly lower degree of H/D exchange between CH_4 and deuterated diethyl ether, even though the barriers for the hydrogen exchange in the **Et*** case are not high.

According to the experimental observations, the H/D exchange between diethyl ether-d_{10} and methane occurs mainly at the β-positions of diethyl ether-d_{10}. An attempt to locate the η^2-H−C(α) complexes was indeed not successful. The optimization gives the O-coordinated TpRu(PH_3)H(OC_4H_{10}) complex when we start with the η^2-H−C(α) complexes. The result suggests that coordination of the η^2-H−C(α) bond creates more steric repulsion and H/D exchange at the α-positions in diethyl ether-d_{10} is expected to be unfavorable. In contrast, the H/D exchange between THF-d_8 and methane occurs preferentially at the α-positions. We believe that the steric arguments can also be applied here. The conversion of the stable O-coordinated (metal-THF) complex to an η^2-H−C species, a precursor complex for C−H bond activation, occurs more easily at the α-positions than at the β-positions.

(b) Structures for the Species Involved in Hydrogen Exchange Processes. Structural details of the optimized intermediates (**1** and **3**) and transition states (**2** and **4**) with their energies relative to those of the σ-complexes **1** in pathways **Ph**, **Et***, and **Me** are shown in Figure 3. The σ-complexes **1Ph**, **1Et***, and **1Me** are calculated to have a distorted octahedral geometry. In comparison to the C−H bonds of free benzene, diethyl ether, and methane, the η^2 H−C bonds in **1Ph**, **1Et***, and **1Me** are 0.039, 0.032, and 0.030 Å longer, respectively.

Structures **2Ph**, **2Et***, and **2Me** are calculated to be the transition states for the transformation of TpRu(PH_3)H(η^2-H−R), **1**, to TpRu(PH_3)R(η^2-H_2), **3**. These transition structures can be approximately described as pentagonal-bipyramidal in which the two hydrides, the alkyl (or phenyl), and two N-donor ligands form the equatorial plane. Examining the distance between the two hydrides and the distance between the metal-bonded carbon in the alkyl (or phenyl) group and its adjacent hydride for each transition structure, we can consider that the transformation (**1** to **3**) occurs via an oxidative addition transition state **2**. Similarly, Chaudret et al. have shown, with the aid of DFT calculations, that the ruthenium(IV) species generated by oxidative addition of the agostic C−H of the phenylpridine ligand in the complex [RuH(H_2)(o-C_6H_5py)(P^iPr_3)$_2$]$^+$ is indeed the transition state in the reversible proton transfer from the agostic C−H to the hydride ligand to form [Ru(H_2)$_2$(o-C_6H_4py)(P^iPr_3)$_2$]$^+$.[14]

In Figure 1, it can be seen that the transformation from **1** to **3** for the benzene case has the smallest barrier

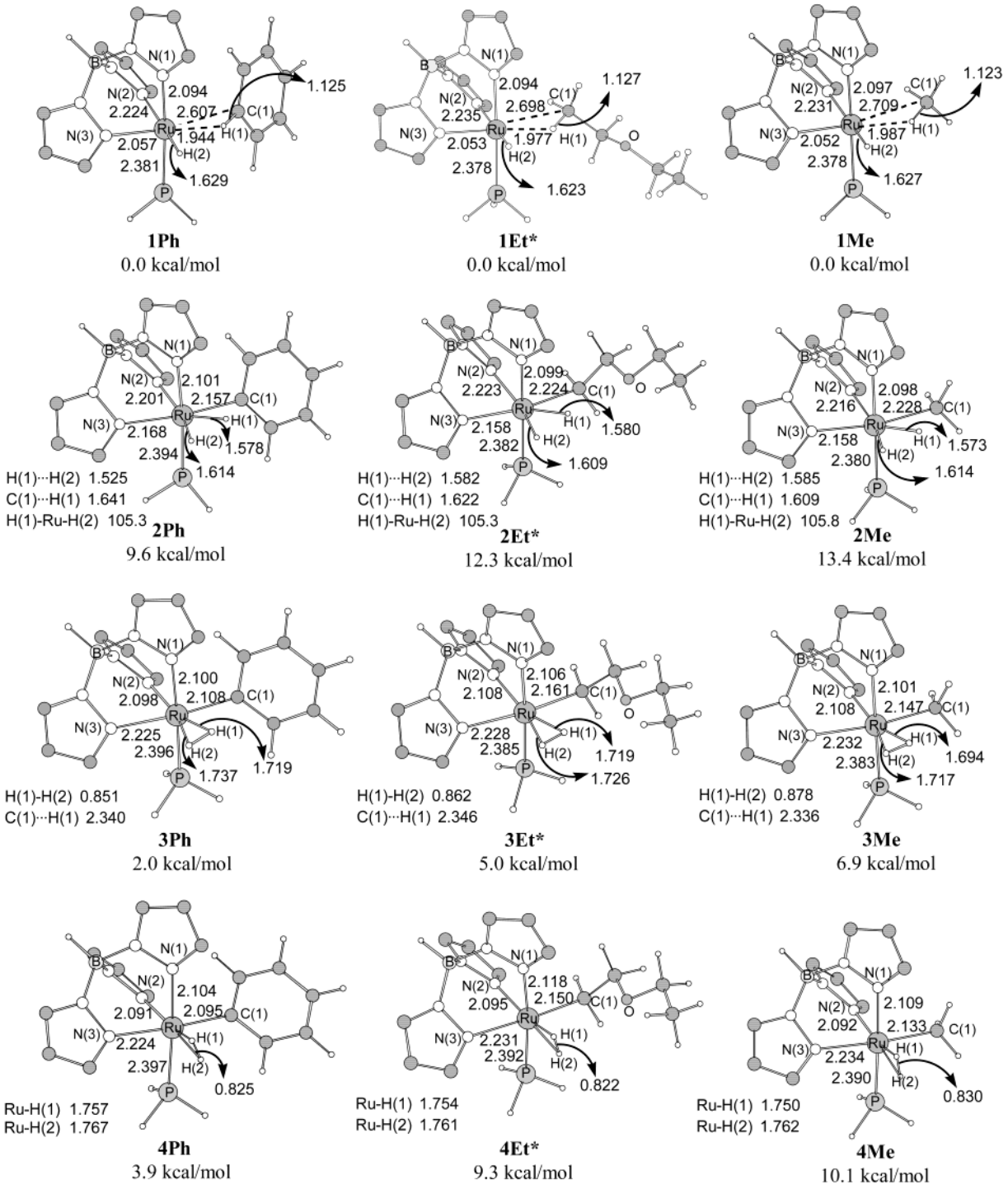

Figure 3. B3LYP optimized structures of η^2-H−C species **1**, transition states **2**, dihydrogen intermediates **3**, and dihydrogen rotational transition states **4** with their selected bond distances and relative reaction energies. Hydrogen atoms on the pyrazolyl ring are omitted. The bond distances and angles are given in Å and deg.

among the three systems studied. From the calculated transition structures (**2Ph**, **2Et***, and **2Me**) shown in Figure 3, the smallest barrier for the benzene case can be traced to the stronger Ru−C(sp^2) bond in the transition structure **2Ph**. The Ru−C(sp^3) bonds in **2Et*** and **2Me** are apparently longer. The methane and ether cases have comparable barriers for the transformations, although a slightly lower barrier is found for the ether case.

The intermediates **3Ph**, **3Et***, and **3Me** are dihydrogen complexes having octahedral structures. The relative stabilities of these three dihydrogen complexes are closely related to the Ru−alkyl (or phenyl) bonding. **3Ph**, having Ru−C(sp^2), is the most stable. In each of these octahedral structures, the η^2-H_2 ligand prefers having the H−H vector orienting parallel to the Ru−C bond. The adopted orientation of the H−H vector gives the optimal metal(d)-to-H_2(σ^*) back-bonding interaction.[25] In addition, the attractive interaction between the metal-bonded carbon of the alkyl (phenyl) group and the neighboring H of the η^2-H_2 ligand is also anticipated to be responsible for the preferred orientation. Similar to the *cis*-effect used to describe the hydride-η^2-H_2 attractive interaction in complexes containing both

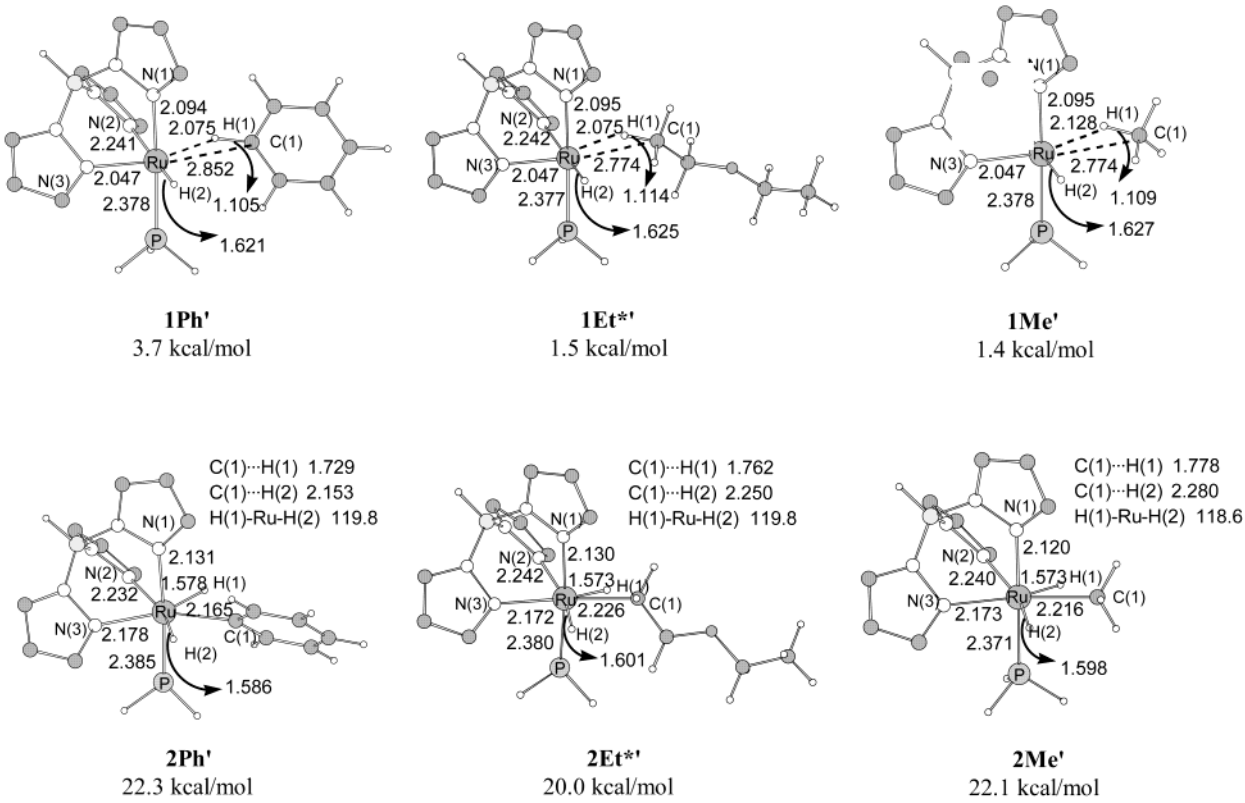

Figure 4. Selected structural parameters of B3LYP optimized η^2-H−C species **1′** and transition states **2′** in Scheme 5 and their reaction energies which are relative to σ-complexes **1** in Scheme 4. Hydrogen atoms on the pyrazolyl ring are omitted.

hydride and η^2-H_2 ligands,[25] the attractive interaction is a result of the orbital interaction between the occupied Ru−C σ-bonding orbital and the unoccupied H−H σ*-antibonding orbital.

The barrier of the η^2-H_2 rotation for the benzene case is again the smallest (1.9 kcal/mol). For the ether case, the rotation has the highest barrier (4.3 kcal/mol). The stronger Ru−C(sp^2) bonding in the benzene case weakens the *cis* attractive interaction between the carbon and the neighboring H of the η^2-H_2 ligand, therefore facilitating the rotation of the dihydrogen molecule. The η^2-H_2 rotation barrier of $TpRh(H)_2(\eta^2\text{-}H_2)$, a Tp-related system, was found to be smaller than 1.0 kcal/mol.[25e] That both hydride ligands in the Rh complex are capable of having the *cis* attraction may be responsible for the small rotation barrier.

(c) Other Considerations and Comments on the H/D Exchange between H_2 and Deuterated Solvents. Scheme 5 mentioned above shows a more direct way to accomplish H/D exchange between CH_4 and the deuterated solvents. Differing from the σ-complexes (**1**) considered above, the σ-complexes proposed in Scheme 5 have the structural arrangement in which H(1) and H(2) are separated by the R group. These new σ-complexes (**1Ph′**, **1Et*′**, and **1Me′**) have been calculated and are shown in Figure 4. Interestingly, the relative energies of these new σ-complexes are slightly higher than that of the corresponding complexes, **1Ph, 1Et***, and **1Me**. The higher stability of **1Ph, 1Et***, and **1Me** can also be explained in terms of the *cis*-effect,[25] in which the hydride ligand in each complex prefers to be *cis* to the H end of the η^2-H−R ligand. On the basis of these new σ-complexes, the corresponding transition states **2Ph′**, **2Et*′**, and **2Me′** (also shown in Figure 4) are calculated to be 22.3, 20.0, and 22.1 kcal/mol with respect to **1Ph, 1Et*,** and **1Me**, respectively. These new transition states (**2Ph′**, **2Et*′**, and **2Me′**) are 12.7, 7.7, and 8.7 kcal/mol, respectively, higher in energy than the transition states (**2Ph**, **2Et***, and **2Me**) based on Scheme 4. Clearly, the more direct pathways in Scheme 5 are not favorable in the hydrogen exchange processes. Although we do not have a definite explanation for the instability of complexes **2′** relative to complexes **2**, comparison of the transition structures suggests that the three ligands (two hydrides and one alkyl) occupy more space in complexes **2′** than in complexes **2**. The ligand spread angles (H(1)−Ru−H(2)) in **2Ph′**, **2Et*′**, and **2Me′** are 119.8°, 118.6°, and 119.8°, respectively, while the corresponding angles (C(1)−Ru−H(2)) are 105.3°, 105.3°, and 105.8° in **2Ph**, **2Et***, and **2Me**, respectively. The greater steric repulsion in structure **2′** is expected to weaken the Ru−Tp bonding interactions.

The rotation of the η^2-H−CH_3 ligand connecting **1Me** to **1Me′** has also been studied. Locating the transition states that correspond to the rotation from **1Me** to **1Me′** is rather difficult, as CH_4 has relatively weak binding to the metal center. Instead of locating the rotational transition states, we scan the potential energy curve by partially optimizing structures having different H(1)−C(1)−Ru−P dihedral angles based on structure **1Me**. The results show that the rotational barriers are within 2.5 kcal/mol. From these calculations, we expect that the rotation of the η^2-H−R ligands in complexes **1** and **1′** can occur freely, although the benzene case is expected to have a higher rotation barrier.

Experimentally, it has been observed that the H/D exchanges occur between H_2 and the deuterated solvents in the presence of $TpRu(PPh_3)(CH_3CN)H$. Calculations show that dihydrogen complexes $TpRu(PH_3)(\eta^2\text{-}H_2)R$ ($R = C_6H_5$, $CH_2CH_2OC_2H_5$, or CH_3) (**3**, see Figures 1 and 3) are intermediates in the H/D exchanges among different organic molecules. It is therefore expected that H_2 can also H/D exchange with deuterated organic solvents. Scheme 6 provides an adequate description of how the H/D exchanges occur.

All the results of our calculations suggest that C−H/C−D activation in the H/D exchange reaction occurs through an oxidative addition pathway. The species resulting from the oxidative addition steps are the relevant transition states in the ruthenium systems studied. A four-center σ-bond metathesis mechanism does not play a role in the activation process.

Conclusion

As part of our research program on activation of H−A (A = H, Si, C, and B) bonds in isolobal ligands H−H, H−SiR′$_3$, H−CR′$_3$, and H−BR′$_2$·L by the metal fragment [Tp(PPh$_3$)RuH], we have studied reactions of CH_4 with $TpRu(PPh_3)(CH_3CN)H$ in various deuterated organic solvents. Unlike the reactions of $TpRu(PPh_3)(CH_3CN)H$ with H_2 and HSiR′$_3$, which yield the isolable σ-complexes, $TpRu(PPh_3)(\eta^2\text{-}H_2)H$ and $TpRu(PPh_3)(\eta^2\text{-}HSiR'_3)H$, respectively, that of $TpRu(PPh_3)(CH_3CN)H$ with CH_4 did not yield any isolable methane σ-complex, nor was it detectable by in-situ NMR study. It was, however, found by NMR and mass spectrometry that $TpRu(PPh_3)(CH_3CN)H$ was capable of catalyzing H/D exchange reactions between CH_4 and the deuterated solvents (R−D); the exchange reactions involved C−H and C−D cleavage of CH_4 and the solvent, respectively. Density functional calculations favor the intermediacies of methane and R−D σ-complexes, $TpRu(PPh_3)(\eta^2\text{-}H\text{-}CH_3)$ and $TpRu(PPh_3)(\eta^2\text{-}D\text{-}R)H$, respectively, in our proposed H/D exchange mechanism. The calculations also show that the two σ-complexes proceed to form the tautomeric η^2-H_2 intermediates $TpRu(PPh_3)(\eta^2\text{-}H_2)(CH_3)$ and $TpRu(PPh_3)(\eta^2\text{-}HD)R$ via oxidative addition pathways, the seven-coordinate species $TpRu(PPh_3)(H)_2(CH_3)$ and $TpRu(PPh_3)(H)(D)R$, respectively, being the transition states, but not intermediates. This is in accord with the fact that the Tp ligand generally enforces an octahedral geometry about the metal center.

Experimental Section

Ruthenium trichloride, $RuCl_3 \cdot 3H_2O$, pyrazole, and sodium borohydride were obtained from Aldrich. Triphenylphosphine was purchased from Merck and was recrystallized from ethanol before use. The complex $TpRu(PPh_3)(CH_3CN)H$ was synthesized according to published procedures.[18] Solvents were distilled under a dry nitrogen atmosphere with appropriate drying agents (solvent/drying agent): tetrahydrofuran/Na-benzophenone, benzene/Na-benzophenone, dioxane/Na-benzophenone, diethyl ether/CaH_2, acetonitrile/CaH_2, hexane/Na. Methane (99.99%) was supplied by Hong Kong Special Gases.

Proton NMR spectra were obtained from a Bruker DPX 400 spectrometer. Chemical shifts were reported relative to residual protons of the deuterated solvents. ^{31}P NMR spectra were recorded on a Bruker DPX 400 spectrometer at 161.70 MHz; chemical shifts were externally referenced to 85% H_3PO_4 in D_2O. High-pressure NMR studies were carried out in commercial 5 mm Wilmad pressure-valved NMR tubes. Mass spectrosopic analyses of the methane and dihydrogen isotopomers resulting from H/D exchanges of CH_4 and H_2 with the deuterated solvents, respectively, were carried out with a Finnigan MAT 95S mass spectrometer.

Catalytic H/D Exchange Reactions between Methane and Deuterated Solvents with $TpRu(PPh_3)(CH_3CN)H$. A 5 mm Wilmad pressure-valved NMR tube loaded with $TpRu(PPh_3)(CH_3CN)H$ (~8 mg) was evacuated and then filled with nitrogen for 3 cycles. Deuterated solvent (0.3 mL) was added to the tube under N_2, and the tube was then pressurized with methane (8 atm). It was heated at 100 °C for 14 h, after which the methane isotopomers in the headspace of the tube were analyzed by mass spectroscopy; the analyses of methane isotopomers deserve special comment.

Analysis of Methane Isotopomers with Mass Spectroscopy. Low-energy electron-impact ionization mass spectra of the methane samples were recorded with a Finnigan-MAT 95S double-focusing magnetic sector mass spectrometer. The instrumental conditions were as follows: electron energy 18.6 eV, ion source temperature 210 °C, mass resolution ($M/\Delta M$) 1000, sample pressure $(1.0-1.5) \times 10^{-6}$ mbar (as recorded by the ion gauge underneath the ionization source), and scan rate 10 s/decade. The kinetic energy of the ionizing electron beam was lowered, and the ionization source conditions were optimized so that little fragmentation from the molecular ion of methane was found. In our hands, the intensity of the m/z 15 fragment was found to be negligibly small at 1.5 ± 0.1% of the base peak at m/z 16 (average ± standard deviation of 5 independent runs spreading over a period of 3 months). Hence, the relative abundance of the CH_4, CH_3D, CH_2D_2, CHD_3, and CD_4 isopotomers could simply be equated to the relative ion intensities of the m/z 16, 17, 18, 19, and 20 peaks, respectively. ^{13}C corrections had been applied to the % methane isotopomers listed in Table 1.

Catalytic H/D Exchange Reactions between H_2 and Deuterated Solvents with $TpRu(PPh_3)(CH_3CN)H$. The exchange reactions were carried out by using the same procedures as for the H/D exchange reactions between CH_4 and deuterated solvents, except that H_2 (10 atm) was used in place of CH_4.

Computational Details. Density functional theory calculations at the Becke3LYP (B3LYP) level[26] have been used to perform the geometry optimizations for all reactants, intermediates, transition states, and products in the hydrogen exchange reactions. Frequency calculations at the same level of theory have also been performed to identify all stationary points as minima (zero imaginary frequency) or transition states (one imaginary frequency). The effective core potentials (ECPs) of Hay and Wadt with double-ξ valence basis set (LanL2DZ)[27] were used to describe Ru and P atoms. For all the other atoms, the standard 6-31G basis set[28] was used except for the uncoordinated C and H atoms in the Tp ligand, where a STO-3G basis set[29] was used. Polarization functions have been added for the C and H atoms ($\xi_p(H) = 1.0$ and $\xi_d(C) = 0.8$) which are directly coordinated to the metal center.

The basis set described above is considered to be small and could be unbalanced. Therefore, it is necessary to test the accuracy by employing a much larger basis set. In the large basis set, polarization functions were added for P ($\xi_d = 0.340$) and Ru ($\xi_f(Ru) = 1.235$)[30] based on Lanl2DZ. The 6-31G** basis set was used for all other atoms. With this much larger basis

(26) (a) Becke, A. D. *J. Chem. Phys.* **1993**, *98*, 5648. (b) Miehlich, B.; Savin, A.; Stoll, H.; Preuss, H. *Chem. Phys. Lett.* **1989**, *157*, 200. (c) Lee, C.; Yang, W.; Parr, G. *Phys. Rev. B* **1988**, *37*, 785.

(27) (a) Hay, P. J.; Wadt, W. R. *J. Chem. Phys.* **1985**, *82*, 270. (b) Wadt, W. R.; Hay, P. J. *J. Chem. Phys.* **1985**, *82*, 284. (c) Hay, P. J.; Wadt, W. R. *J. Chem. Phys.* **1985**, *82*, 299.

(28) Hariharan, P. C.; Pople, J. A. *Theor. Chim. Acta* **1973**, *28*, 213.

(29) Hehre, W. J.; Stewart, R. F.; Pople, J. A. *J. Chem. Phys.* **1969**, *51*, 2657.

set, we performed single-point energy calculations for complexes **1**−**4**. The relative energies (in kcal/mol) using the large basis set are **1Ph** (0.0), **2Ph** (10.0), **3Ph** (2.2), and **4Ph** (3.8), and those obtained with the small basis set are **1Ph** (0.0), **2Ph** (9.6), **3Ph** (2.0), and **4Ph** (3.9). For the methane system, the large basis set gives **1Me** (0.0), **2Me** (14.4), **3Me** (7.6), and **4Me** (10.2), while the small basis set gives **1Me** (0.0), **2Me** (13.4), **3Me** (6.9), and **4Me** (10.1). For the ether system, the relative energies calculated with the large basis set are **1Et*** (0.0), **2Et*** (12.2), **3Et*** (4.5), and **4Et*** (8.1) in comparison to those obtained with the small basis set, **1Et*** (0.0), **2Et*** (12.3), **3Et*** (5.0), and **4Et*** (9.3). All these calculations suggest that the small basis set used in our calculations does not have the unbalanced problem and is able to provide reasonable results in discussing the reaction pathways studied in this paper.

All calculations were performed with the use of the Gaussian 98 package[31] on Silicon Graphics Indigo workstations and PC Pentium III computers.

Acknowledgment. We thank the Hong Kong Research Grant Council (Project Nos. PolyU 5178/99P and HKUST6186/00P) for financial support. We would also like to thank Mr. Y. K. Au and Miss P. S. Chan for technical help in obtaining the mass spectra.

OM0209024

(30) Ehlers, A. W.; Bohme, M.; Dapprich, S.; Gobbi, A.; Hollwarth, A.; Jonas, V.; Kohler, K. F.; Stegmann, R.; Veldkamp, A.; Frenking, G. *Chem. Phys. Lett.* **1993**, *208*, 111.

(31) Frisch, M. J.; Trucks, G. W.; Schlegel, H. B.; Scuseria, G. E.; Robb, M. A.; Cheeseman, J. R.; Zakrzewski, V. G.; Montgomery, J. A., Jr.; Stratmann, R. E.; Burant, J. C.; Dapprich, S.; Millam, J. M.; Daniels, A. D.; Kudin, K. N.; Strain, M. C.; Farkas, O., Tomasi, J.; Barone, V.; Cossi, M.; Cammi, R.; Mennucci, B.; Pomelli, C.; Adamo, C.; Clifford, S.; Ochterski, J.; Petersson, G. A.; Ayala, P. Y.; Cui, Q.; Morokuma, K.; Malick, D. K.; Rabuck, A. D.; Raghavachari, K.; Foresman, J. B.; Cioslowski, J.; Ortiz, J. V.; Baboul, A. G.; Stefanov, B. B.; Liu, G.; Liashenko, A.; Piskorz, P.; Komaromi, I.; Gomperts, R.; Martin, R. L.; Fox, D. J.; Keith, T.; Al-Laham, M. A.; Peng, C. Y.; Nanayakkara, A.; Challacombe, M.; Gill, P. M. W.; Johnson, B.; Chen, W.; Wong, M. W.; Andres, J. L.; Gonzalez, C.; Head-Gordon, M.; Replogle, E. S.; Pople, J. A. *Gaussian 98*, revision A.9; Gaussian, Inc.: Pittsburgh, PA, 1998.